

On the Importance of non-intrinsic dissolution in Nanoparticulate Platinum Electrocatalysts

Primož Jovanovič*^{a,b,‡}, Urša Petek^{a,d}, Nejc Hodnik^c, Francisco Ruiz-Zepeda^a, Matija Gatalo^{a,d}, Martin Šala^b, Vid Simon Šelih^b, Tim Patrick Fellingner^e and Miran Gaberšček*^{a,d}

^aDepartment of Materials Chemistry, National Institute of Chemistry Hajdrihova 19, 1000 Ljubljana, Slovenia

^bDepartment of Analytical Chemistry, National Institute of Chemistry, Hajdrihova 19, 1000 Ljubljana, Slovenia

^cDepartment of Catalysis and Chemical reaction Engineering, National Institute of Chemistry Hajdrihova 19, 1000 Ljubljana, Slovenia

^dFaculty of Chemistry and Chemical Technology, University of Ljubljana, Večna pot 113, SI-1000 Ljubljana, Slovenia

^eMax Planck Institute of Colloids and Interfaces, Colloids Department, Am Mühlenberg 1, Potsdam, Germany

Supporting Information

S1: Specific surface area measurement and pore volume determination

Table S1.1: Total pore volume and BET values of HSANDC support material.

Parameters	
Quenched Solid Density Functional Theory (QSDFT, cylindrical, slit and spherical pores)	
Micropore volume [$\text{cm}^3 \text{g}^{-1}$]	1.2
External surface area [$\text{m}^2 \text{g}^{-1}$]	204
BET surface area [$\text{m}^2 \text{g}^{-1}$]	2335
QSDFT surface area [$\text{m}^2 \text{g}^{-1}$]	1847
Total pore volume [$\text{cm}^3 \text{g}^{-1}$]	1.44
Non-Local Density Functional Theory (NLDFT, slit and cylindrical pores)	
Micropore volume [$\text{cm}^3 \text{g}^{-1}$]	1.2
External surface area [$\text{m}^2 \text{g}^{-1}$]	204
BET surface area [$\text{m}^2 \text{g}^{-1}$]	2335
NLDFT surface area [$\text{m}^2 \text{g}^{-1}$]	1981
Comparison to BMP800 (NLDFT slit and cylindrical pores)	
BET surface area [$\text{m}^2 \text{g}^{-1}$]	320
Micropore volume [$\text{cm}^3 \text{g}^{-1}$]	0.074
Total pore volume [$\text{cm}^3 \text{g}^{-1}$]	0.749

S2: Transmission electron microscopy analysis

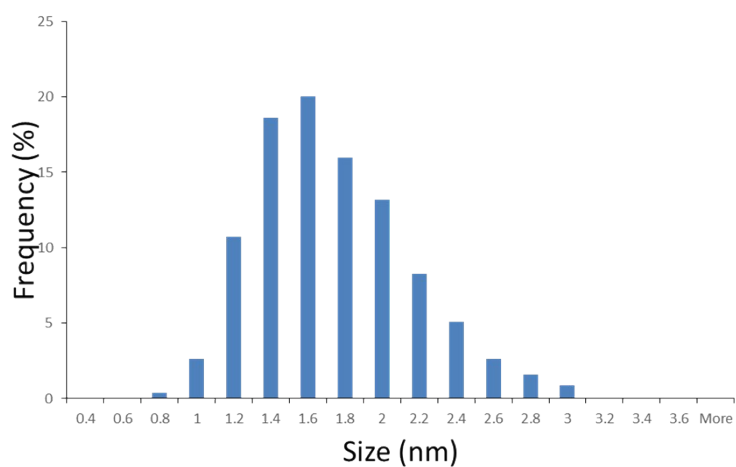


Figure S2.1: Particle size distribution of Pt@HSANDC analogue.

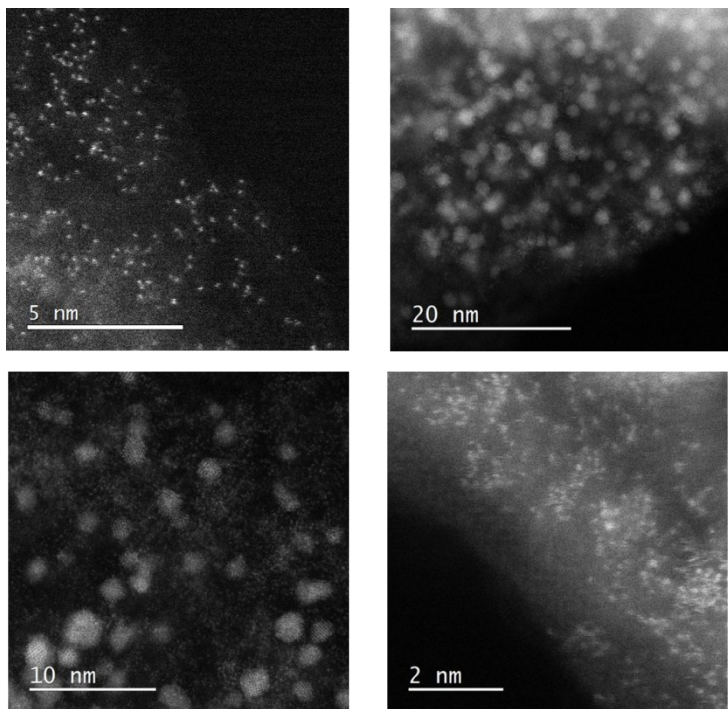


Figure S2.2 TEM analysis of Pt@HSANDC.

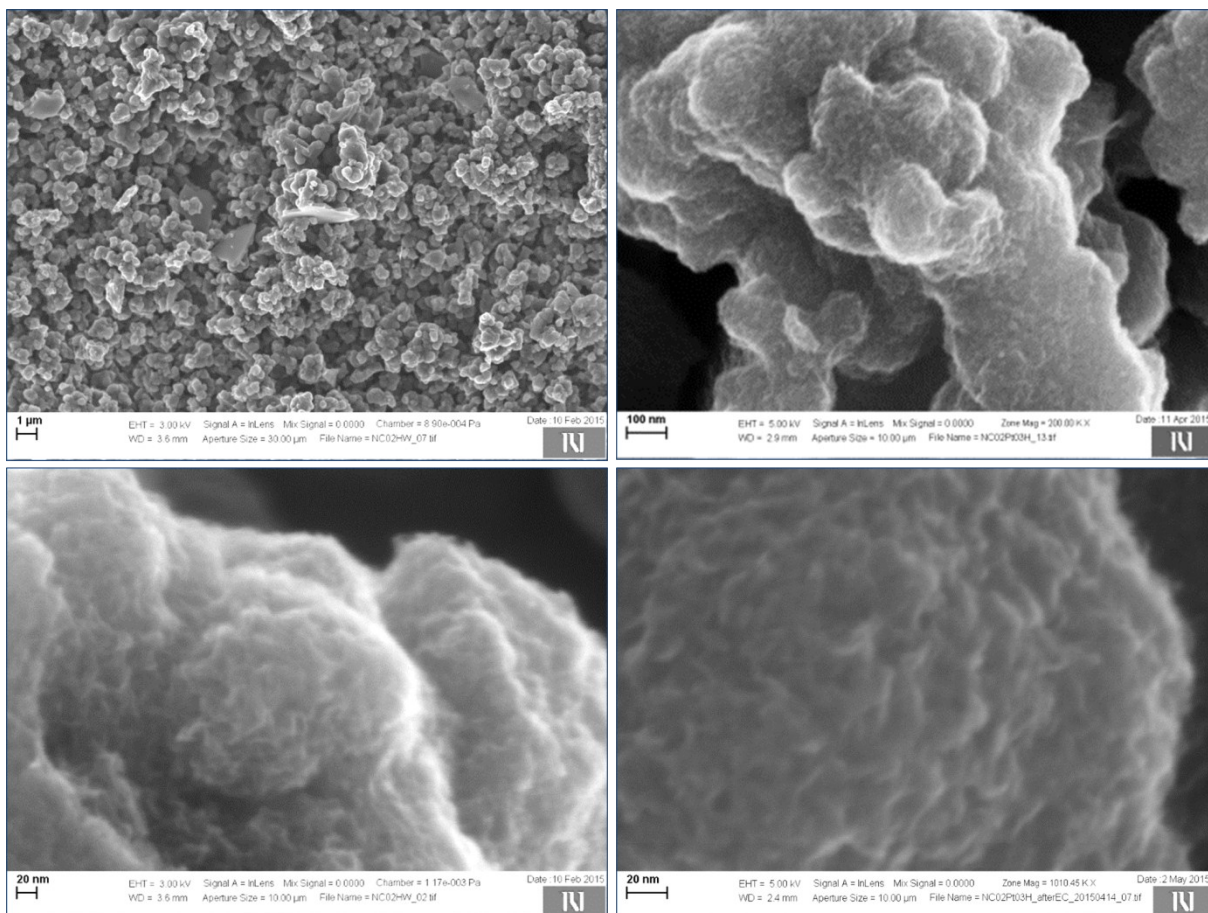


Figure S2.3: SEM analysis of HSANDC support.

S3: Electrochemical flow cell coupled to ICP-MS

S3.1: Dissolution of Pt from Pt/C under slow (5 mVs⁻¹) potentiodynamic regime

In a slow potentiodynamic experiment a typical Pt dissolution profile splits into an anodic and a dominating cathodic dissolution [3,34]. In Fig. S3.1.1 the dissolution profiles of a commercial Pt/C catalyst with different particle sizes (see Table are shown. We note here that the dissolution signal is not normalized per real Pt surface area. In any case, before such normalisation, one should make sure that the thickness of the catalyst layer is sufficiently low in order to avoid the non-intrinsic, oversaturation phenomena [42]. In our case, the dissolution profiles of Pt/C catalyst (Fig. 2.1.1) do not show any overlapping, which would be expected if the non-intrinsic phenomena controlled the dissolution proces. Although the total amount of the catalyst was the same in all present samples, the film thickness was bigger in the case of Pt/C 1 nm due to the lower metal loading. Hence the carbon content was also bigger in this case (see Table 1 in the main text). In the case of the other two analogues (Pt/C 2.6 nm and Pt/C 4.8 nm) the film thickness was approximately the same since the Pt content was similar. Therefore, it is reasonable to conclude that the differences in dissolution profiles of Fig. S3.1.1 are due to the intrinsic stability differences, which in turn are a consequence of the particle size effect [3,40,43–47].

Since the intrinsic nature of dissolution obviously prevailed over the non-intrinsic phenomena in this particular experiment, the data could be normalized per real Pt surface area (Fig. S3.1.2). As expected based on several previous reports [3,39,40,43–47], the dissolution rate decreases as the particle size is increased. A detailed inspection of dissolution profiles reveals that in the case of the smallest nanoparticles (Pt/C 1 nm) the overall dissolution rate is much more intense: the dissolution sets on already around 0.564 V vs RHE in the anodic scan, which is approximately 340 mV less positive in comparison to the other two analogues (Fig. S3.1.2a). This trend is in agreement with the theoretical and experimental findings by Tang et al who showed that the dissolution potential shifted to positive potentials with increasing particle size [43,44]. Furthermore, in those studies it was shown that the dissolution mechanism was particle size dependent as well. Namely, in the case of small particles the dissolution occurs via a direct path (Pt to Pt²⁺), as the surface is not passivated with oxo species. In the case of bigger particles (~ 4 nm) the dissolution starts at higher potentials and proceeds through an oxide formation path that induces the so called place exchange mechanism [48]. In our case this could explain the experimental results observed when

cycling into the Pt oxide formation region – i.e. above 1 V (Fig. S3.1.2 b-d). In that case the dissolution was detected also in the case of the largest particles (4.8 nm). In the intermediate case (Pt 2.6 nm), however, a well resolved dissolution is noticed already when cycling till 1 V. This indicates that direct dissolution is also taking place on particles of this size. In case of 4.8 nm analogue the direct dissolution is barely visible, therefore this could be the approximate limiting boundary for the predominantly direct dissolution mechanism. This result is in line with Tang et al [43,44]. We note that in the case of the same 4.8 nm Pt/C catalyst dissolution has been detected by Cherevko et. al by using similar analytical approach as in the present manuscript [4]. Furthermore, the dissolution trend in Fig. 3.1.2 is also in agreement with the Gibbs-Thomson energy trend which increases with decreasing particle size [46]. Additionally, one has to take into account the concentration of low coordinated Pt surface atoms which increases with decreasing particle size [45,46]. Also, low coordinated atoms are more oxophilic [49]. Due to this formation of oxide and subsequent place-exchange most likely proceeds at lower potentials than in the case of larger particles [6]. Overall, the understanding of Pt dissolution onset has not been completely elucidated so far. Nevertheless, from the dissolution data (Fig. S3.1.2) it can be concluded that under slow (5 mVs^{-1}) potentiodynamic conditions the particle size effect is the dominating phenomenon controlling the corrosion of Pt nanoparticles dispersed on commercial carbon supports.

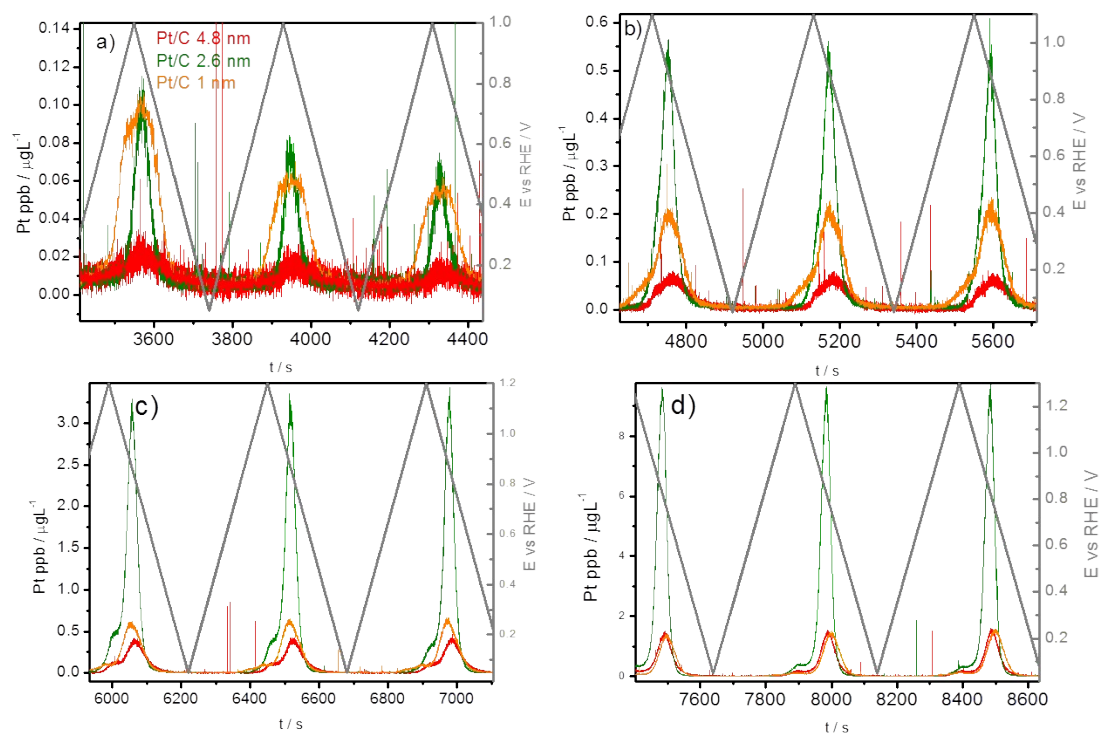


Figure S3.1.1: Time and potentially resolved dissolution profile during slow potentiodynamic experiment.

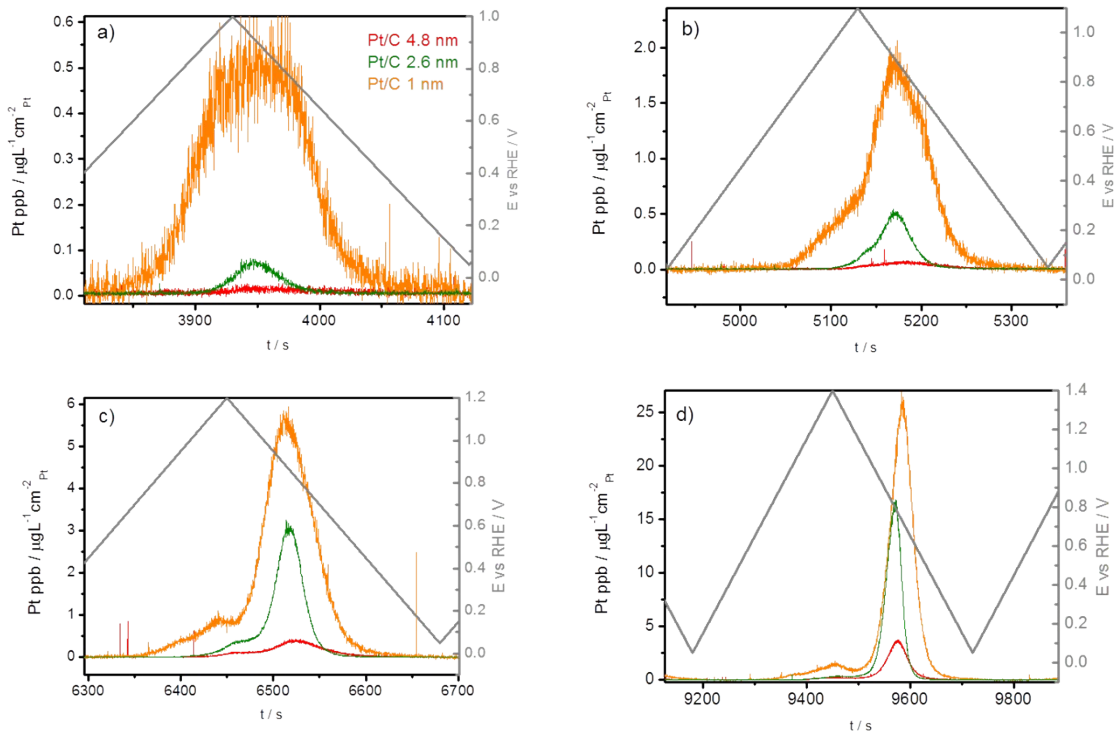


Figure S3.1.2: Time and potentially resolved dissolution profile normalized per real Pt surface area during slow potentiodynamic experiment by gradually increasing UPL: a) 1.0 V, b) 1.1 V, c) 1.2 V and d) 1.3 V.

The platinum surface area used for normalization of dissolution profiles in Fig. S3.1.2 was determined by charge integration of hydrogen under potential deposition (HUPD) region. The percentage of dissolved Pt in investigated samples is shown in Fig. S2.1.3.

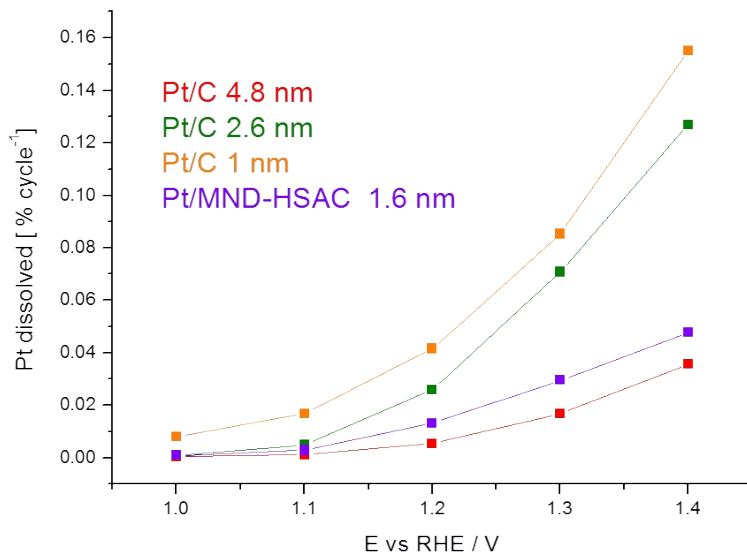
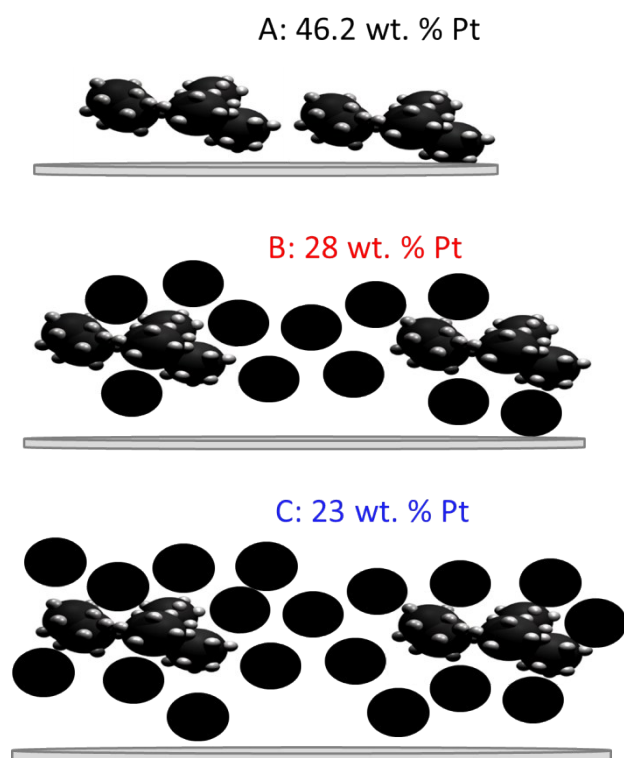


Figure S3.1.3: Percentage of dissolved Pt at different UPLs in case of different catalysts.

S 3.2 Preparation of Pt/C (2.6 nm) catalyst films with different carbon loadings

In the case of different carbon loadings, potentiodynamic experiments were performed in the same manner as described in the main text. Electrodes with different carbon loadings were prepared as follows:

First a suspension of Pt/C (2.6 nm) catalyst was prepared so that the total mass concentration of the catalyst was $1 \mu\text{g}/\mu\text{L}$ (indexed with A). A second suspension (suspension B) was prepared in the same way as A except that 1.72 mg of Vulcan carbon was added which corresponded to a 124 % increase relative to the mass of carbon in suspension A. A third suspension (suspension C) was prepared in the same way by adding 2.75 mg of Vulcan - a 194 % increase in mass of carbon relative to suspension A. In all cases the volume of Mili Q water was kept the same (2.63 mL) hence the concentration of Pt was the same. Therefore the mass of platinum on the electrode was the same in all cases and only the mass of carbon was varied.



Scheme S3.2.1: Schematic presentation of catalyst films with different Pt:C ratios.

S4: Rotating disc electrode measurements

S 4.1 Activity measurement

Electrochemical measurements were conducted in a two compartment electrochemical cell in a 0.1 M HClO₄ (purity > 99.99 %, Aldrich) electrolyte with conventional three electrode system controlled by a potentiostat (Compact stat, Ivium technologies). Ag/AgCl was used as a reference and a Pt wire as a counter electrode. The working electrode was a glassy carbon disk embedded in Teflon (Pine Instruments) with a geometric surface area of 0.196 cm². Prior to each experiment, the electrode was polished to mirror finish with Al₂O₃ paste (particle size 0.05 μm, Buehler) on a polishing cloth (Buehler). After polishing the electrodes were rinsed and sonicated in a 18 MΩcm⁻¹ mili-Q water for 5 minutes. 20 μL of 1 mgmL⁻¹ water based, well dispersed catalyst ink was pipetted on the glassy carbon electrode completely covering it and dried under different conditions, as explained further in the text. Such preparation resulted in a loading of approximately 25 μgPtc⁻². After drying the electrode was mounted on the rotator (Pine Instruments). The electrode was placed in Ar saturated electrolyte under potential control at 0.05 V vs RHE. The catalysts were electrochemically activated for 200 cycles between 0.05 V and 1.2 V (vs. RHE) with a scan rate of 300 mVs⁻¹. ORR polarization curves were measured in an oxygen saturated electrolyte with rotation at 1600 RPM in the same potential window with a scan rate of 20 mVs⁻¹. After subtraction of background current due to capacitive currents, the kinetic parameters were calculated at 0.9 V. Ohmic resistance of the electrolyte was determined and compensated for as reported in ref. [2]. Electrochemical surface area (ECSA) was determined in a CO stripping experiment as described in the literature [3,4]. All potentials are given against the reversible hydrogen electrode (RHE). The values of RHE were determined by measuring open circuit potentials (OCP) in a H₂ saturated electrolyte.

Table S4.1.1: Electrochemical RDE characterization.

Sample name	ESA CO [m ² /g _{Pt}]	Spec. Activity [mA/cm ²]	Mass Activity [mA/mg _{Pt}]
Pt@HSANDC	47	0.54	0.26
Pt/C-1 nm	116	0.41	0.47
Pt/C-2.6 nm	99	0.38	0.37
Pt/C-4.8 nm	56	0.46	0.26

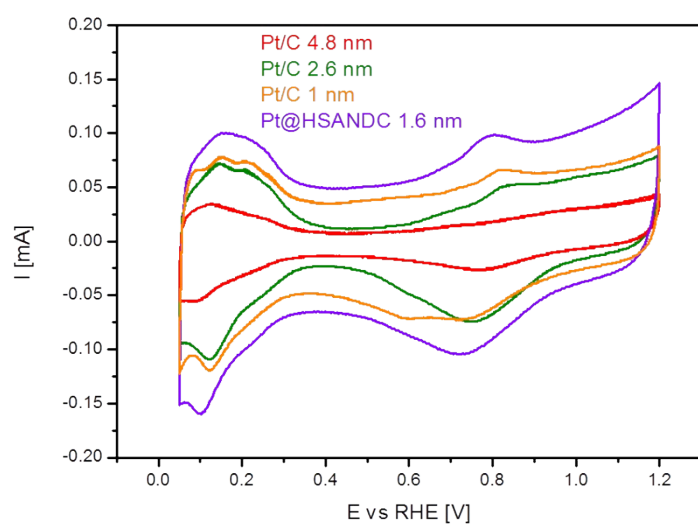


Figure S4.1.2: Representative CVs of investigated samples.

S 4.2 Comments on ESA values for the Pt@HSANDC analogue

According to the small average particle size one would expect a higher ESA value (around 100 m²/g_{Pt}) as reported in the literature for particles of similar sizes. The lower ESA value in the present case is ascribed to the presence of Pt single atoms (see Fig. S2.2) which are electrochemically inactive. Abundance of the single atoms is ascribed to the low annealing

temperature (400 °C) during the synthesis procedure. Additionally, some parts of particles are covered/blocked by carbon support (some particles are strongly embedded in carbon).

References

- [1] A.A. Topalov, S. Cherevko, A.R. Zeradjanin, J.C. Meier, I. Katsounaros, K.J.J. Mayrhofer, Towards a comprehensive understanding of platinum dissolution in acidic media, *Chem. Sci.* 5 (2014) 631–638. doi:10.1039/c3sc52411f.
- [2] D. van der Vliet, D.S. Strmcnik, C. Wang, V.R. Stamenkovic, N.M. Markovic, M.T.M. Koper, On the importance of correcting for the uncompensated Ohmic resistance in model experiments of the Oxygen Reduction Reaction, *J. Electroanal. Chem.* 647 (2010) 29–34. doi:10.1016/j.jelechem.2010.05.016.
- [3] K.J.J. Mayrhofer, D. Strmcnik, B.B. Blizanac, V. Stamenkovic, M. Arenz, N.M. Markovic, Measurement of oxygen reduction activities via the rotating disc electrode method: From Pt model surfaces to carbon-supported high surface area catalysts, *Electrochim. Acta.* 53 (2008) 3181–3188. doi:10.1016/j.electacta.2007.11.057.
- [4] Y. Garsany, O.A. Baturina, K.E. Swider-Lyons, S.S. Kocha, Experimental methods for quantifying the activity of platinum electrocatalysts for the oxygen reduction reaction., *Anal. Chem.* 82 (2010) 6321–8. doi:10.1021/ac100306c.